Int. J. Electrochem. Sci., 10 **(2015)** 10145 - 10156

International Journal of
ELECTROCHEMICAL
SCIENCE
www.electrochemsci.org

Scanning Electrochemical Microscopy Studies for the Characterization of Localized Corrosion Reactions at Cut Edges of Painted Galvanized Steel as a Function of Solution pH

B.M. Fernández-Pérez[1], *J. Izquierdo*[1,2], *J.J. Santana*[3], *S. González*[1], *R.M. Souto*[1,2,*]

[1]Department of Chemistry, University of La Laguna, P.O. Box 456, E-38200 La Laguna, Tenerife, Canary Islands, Spain.
[2]Instituto Universitario de Materiales y Nanotecnologías, University of La Laguna, E-38200 La Laguna, Tenerife, Spain
[3]Department of Process Engineering, University of Las Palmas de Gran Canaria, E-35017 Las Palmas de Gran Canaria, Gran Canaria, Spain
[*]E-mail: rsouto@ull.es

Received: 7 April 2015 / *Accepted:* 4 May 2015 / *Published:* 4 November 2015

Coil coated steel sheets immersed in 1 mM NaCl solutions adjusted at both acidic and alkaline pH conditions were used to investigate the cut edge corrosion behaviour by scanning electrochemical microscopy. Combined amperometric/potentiometric operation revealed asymmetries in the distribution of localized anodic and cathodic activities along the cut edge related to the onset of a differential aeration mechanism. The anodic activity was initially located at the aluzinc layer coated with the thinner organic coating, whereas alkalization of the steel foil related to cathodic activity was limited by the buffering ability of the soluble metal ions. In this way, precipitation of corrosion products might block the cathodic sites, a process responsible for the eventual complete cessation of corrosion in alkaline solution for sufficiently long exposures.

Keywords: SECM; corrosion at edges; concentration distributions; zinc; steel; pH effects.

1. INTRODUCTION

Metal exposed at cut edges often constitutes the mode of failure of steel-based materials protected against corrosion by polymer coatings. Even active corrosion protection by depositing layers of less noble metals such as zinc results insufficient in this case, due to the big difference in dimensions between the steel matrix and the metallic and polymeric layers. In this way, there is a limited amount of sacrificial metal available for the sacrificial protection of the material. Therefore, mechanistic investigation of cut edge corrosion remains an important issue towards developing more

efficient metal/coating systems with greater corrosion resistance. In this effort, scanning microelectrochemical techniques are gaining special interest as they collect chemical information with high spatial resolution while operating *in situ*. Among them, current density mapping using the scanning vibrating electrode technique (SVET) has been especially suited because it allowed to locate the corrosion sites related to both anodic and cathodic half-cell reactions. Furthermore, real time operation facilitates the progress of corrosion related to its growth or repassivation to be observed. In this way, the major influence of oxygen permeability in promoting the delamination of the polymeric coating as result of the scavenging dissolution of the sacrificial metallic layers has been demonstrated by Worsley and coworkers [1,2]. Preferential dissolution of the zinc layer resulting from differential aeration was observed when polymer coating layers of either different thickness [3] or different porosity [4] were applied on the two sides of galvanized steel. Very interestingly, the differential aeration mechanism could be compensated by inclusion of anodic inhibitor species in the primer layer adjacent to the thicker coating and cathodic inhibitors in the primer layer beneath the thinner coating [5]. This feature confirms previous observations by SVET of localisation in the anodic activity at the cut edge due to variations in the concentration of the inhibitor species in the organic coatings applied on either side [6].

By coupling current density and pH mapping, local differences in pH and variations in the electrochemical activity along the cut edge could be related by Ogle et al. [7,8] to the formation of inhibiting films. Large pH variations were observed in the solution adjacent to the cathodic sites formed on the steel substrate, ranging from near neutral to above 10, as result of the formation of hydroxide ions according to equation (1):

$$O_2 + 4e^- + 2H_2O \rightarrow 4OH^- \quad (1)$$

Corrosion product precipitation would eventually result as released Zn^{2+} ions from the anodic sites would encounter the more alkaline environment, and they can affect the rate of corrosion by either blocking the reacting cathodic surface [7-9] or the rate of oxygen reduction [10]. The extent of the inhibitive effect would be influenced by surface area ratio and geometry [11,12], and the amount of electrolyte over the galvanic couple [12]. Conversely, no evidence of acidification due to metal dissolution and hydrolysis through equations (2) and (3) was found in their work [7]:

$$Zn \rightarrow Zn^{2+} + 2e^- \quad (2)$$

$$Zn^{2+} + H_2O \rightarrow Zn(OH)^+ + H^+ \quad (3)$$

However, reports on local acidification around the anodic sites on painted cut edges were recently given by Alvarez-Pampliega et al. [14], and the extent of the acidification effect was related to the amount of aluminium in the zinc metallic layer applied on steel. In the case of pure zinc galvanization, anodic dissolution of Zn^{2+} led to pH values varying between 5.0 and 6.2 around the anodic sites, values significantly lower than those reported by Ogle and coworkers [7]. The occurrence of acidification around painted cut edges has also been proposed by Lowe et al. [15]. They conducted a systematic investigation of pH effects around a cut edge related to the release of soluble metal ions from the metal coating. By using a multiband electrode configuration allowing separate monitoring of the steel and metal coating layers, pH variations related to the presence of Zn^{2+} and Al^{3+} ions could be established. In this way, acidification of the system occurred when these metal ions were present in the

solution, and the effect was more pronounced in the case of the latter leading to an increase in the corrosion rates. Furthermore, strong buffering effects due to these metal ions were also reported [15], whereas the precipitation of corrosion products due to the high alkaline pH values developed close to the steel strip may block the cathodic sites [7,16], thus effectively decreasing the corrosion rate in the system. It must be noticed here that buffering effects on the corrosion rate due to precipitation of corrosion products in a painted cut edge were already described by Ogle and coworkers in 2000 [7], though they inferred these effects to hinder solution acidification around the anodic sites. Therefore, the effect of dissolving Zn^{2+} ions on the local pH around a galvanized cut edge remains controversial.

Local differences in chemical activity related to corrosion processes can be visualized in situ using the scanning electrochemical microscope (SECM) (a detailed review on the uses and applications of SECM in corrosion science is given in ref. [17]). In this technique, the SECM probes can be rastered in closer proximity to the investigated surfaces, and can be made to be electrochemically selective in their response, thus providing greater chemical resolution [18]. In particular, the combined amperometric/potentiometric operation has become a powerful tool to gain new insights in the corrosion mechanism of magnesium-based materials [19-21], the spatial distribution of reacting sites in galvanic corrosion reactions [22-24], and the inhibitive effect of organic inhibitors on the corrosion of reactive metals [25]. Therefore, this experimental approach can be regarded a powerful new route for the investigation of the local effects operating during the corrosion of painted cut edges. In a recent publication, the applicability of the method was demonstrated in a study of the localized corrosion reactions occurring at cut edges of coil-coated steel exposed to naturally aerated 1mM NaCl solution. In addition to the test of principle, preliminary experiments showed that differential aeration processes could be spatially-resolved also in the case of organic coated cut edges when coatings of different thickness were applied at either side of the sample [26]. Additionally, the local variation of pH at the anodic sites due to metal dissolution and hydrolysis, with the production of acidification due to the co-dissolution of zinc and aluminium from the aluzinc metallic layers, was monitored.

This study was undertaken in view to investigate the effect of solution pH on the relative contributions of metal dissolution and hydrolysis, the eventual occurrence of associated buffering effects, and the impact of corrosion product precipitation associated to the degradation of coil coated steel (CCS) from cut edges. This study is an extension of the previous work conducted for an asymmetric CCS immersed in chloride-containing aqueous solution under near neutral conditions [26]. In this case, both acidic and alkaline conditions were imposed to the bulk electrolyte solution to modify the relative contribution of the different processes involved in the corrosion reaction. The lower pH value was chosen because zinc oxides cannot precipitate though corresponding to acid rain conditions, whereas the opposite occurs in the solution of higher pH [27].

2. EXPERIMENTAL

Coil-coated steel (CCS), consisting of 0.4 mm mild steel foil galvanized with 20 μm thick aluzinc layers (nominal composition of 55% zinc and 45% aluminium), and coated with a polyester

paint, was considered for the investigation. The paint layers consisted of 5 μm thick primer containing strontium chromate applied to either side of the metallic samples, and covered with a single 20 μm thick topcoat containing TiO_2 on one side. The samples were embedded in an epoxy resin, so that only the cross section (approximately 2 mm length and 450 μm width) was exposed to the test environment. During SECM scanning, the zinc layer with the top coat was placed at the right side. The mount with the samples was polished using silicon carbide paper down to 4000 grit and then alumina of 0.3 μm particle size, washed thoroughly with 96% ethanol, and dried in air. The mount was surrounded laterally by Sellotape creating a container for approximately 3.5 mL of electrolyte solution, thus exposing the cut edge upwards. Tests were conducted in 1 mM NaCl solution, naturally aerated, at ambient temperature. The effect of pH of the test environment on the corrosion processes occurring at the cut edge was investigated by adding either HCl to bring the pH down to 4.2, or NaOH to produce an alkaline environment of pH 9.8 in the 1 mM NaCl solution. These additions caused only a minor change in the concentration of the chloride ions.

Measurements were performed in an SECM equipment built by Sensolytics (Bochum, Germany), using an Autolab bipotentiostat provided with a frequency response analyzer (Metrohm, Herisau, Switzerland) as electrochemical interface. The electrochemical cell was completed with an Ag/AgCl/(3 M) KCl reference electrode, and a Pt wire as counter electrode. Two different operation modes were employed in this work, namely potentiometric using an antimony tip, and amperometric using a platinum microdisk. Potentiometric operation was attained using an antimony microelectrode with 40 μm diameter active disk surface, which exhibited a linear relationship between the potential and the solution pH in the $3 < pH \leq 11$ range, with slope 48.2 mV/pH unit. Details on the fabrication of the antimony microelectrode and its calibration are described elsewhere [28]. For the potentiometric measurements, a home-made voltage follower based on a 10^{12} Ω input impedance operational amplifier was interconnected between the cell and the potentiometric input. Alternately, a platinum microdisk of diameter 10 μm was employed in the amperometric operation of the SECM. In this case, ferrocene-methanol of concentration 0.5 mM added to the electrolyte solution acted as electrochemical mediator at the tip (feedback mode). The tip potential was held at +0.50 V vs. Ag/AgCl/(3 M) KCl to enable the diffusion-limited oxidation of ferrocene-methanol to ferrocinium ions. In both cases, SECM measurements were performed over the cut edge at a height of 15 μm with a scan rate of 7 μm s^{-1}.

3. RESULTS AND DISCUSSION

The location and the dimensions of the active sites developing at the cut edge during immersion in naturally-aerated 1 mM NaCl solutions of varying pH can be imaged using the SECM in either amperometric or potentiometric modes by using a suitable tip microelectrode. The advantage is that no polarization of the substrate is required, thus the system corrodes spontaneously in the environment while scanned by the tip. The positive potential value required for the oxidation of ferrocene-methanol (namely, +0.50 V vs. Ag/AgCl/(3 M) KCl) hindered the use of the antimony tip for amperometric operation, and it was only employed to monitor local pH distributions potentiometrically. Amperometric operation was performed using a platinum tip. In this way, the concentration

distributions of various species participating in the corrosion reactions could be imaged in a single experiment. The SECM data were drawn using the dimensionless current (i / i_{lim}), where i_{lim} is the limiting current when the tip is far away from the surface.

3.1. SECM imaging of the cut edge in acid environment (pH 4.2)

Figures 1 and 2 show the faradaic current measured at the tip for ferrocene-methanol oxidation and the pH distribution sensed at the SECM tips as they were travelling above the cut edge. They were taken at different elapsed times since the sample was put in contact with the acidified 1 mM NaCl solution. Electrochemical activity is observed to occur both over the mild steel foil and the two metal-coated layers at each side, as it should be expected for a system where the different metals are in direct contact and experience the same electric potential. The corrosion reaction appears to occur initially at a faster rate with the elapse of time, as shown by the progressive increase in the measured feedback currents. No blocking of the corroding surface can occur at this pH because the most stable species formed at pH values smaller than 5 is the Zn^{2+} ion [27]. A more detailed observation of the evolution of the current plots with the elapse of time allows noticing that the increase of electrochemical activity does not occur in the same extent over all the cut edge. In fact, the shape of the current plots become asymmetrical with the elapse of time, indicating that higher availability of electrons for redox mediator regeneration occurs around the steel/metal coated layer interface situated at the right. This corresponds to the aluzinc layer that was coated with the thickest polymeric coating.

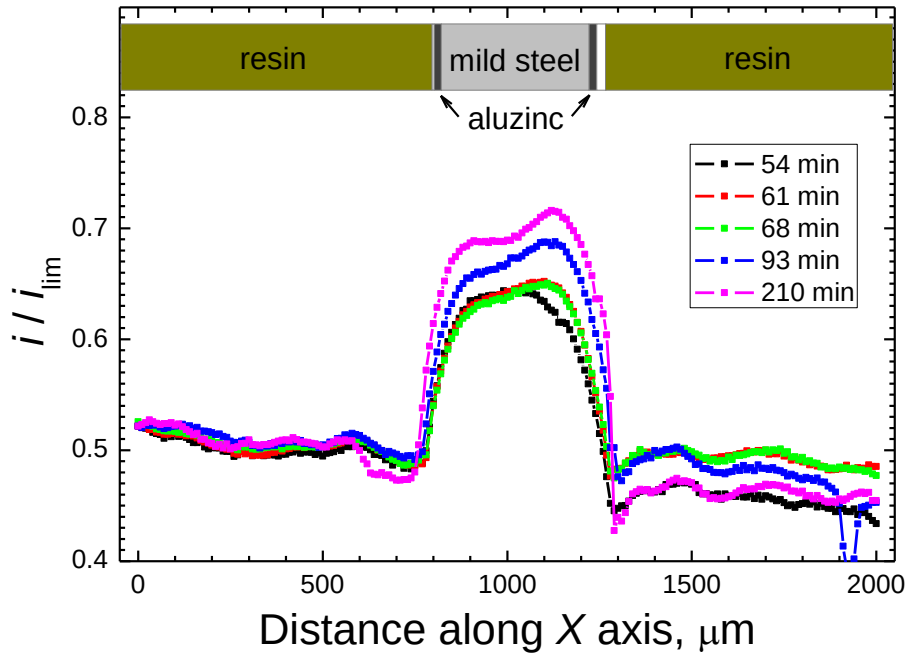

Figure 1. Distribution of electrochemical activity towards regeneration of ferrocene-methanol over a CCS cut edge immersed in 1 mM NaCl (pH 4.2) measured by amperometric SECM using a platinum tip for immersion times indicated in the graph. E_{tip} = +0.50 V vs. Ag/AgCl/(3 M KCl); tip-substrate distance: 15 μm; tip diameter: 10 μm. Scan rate: 7 μm s^{-1}.

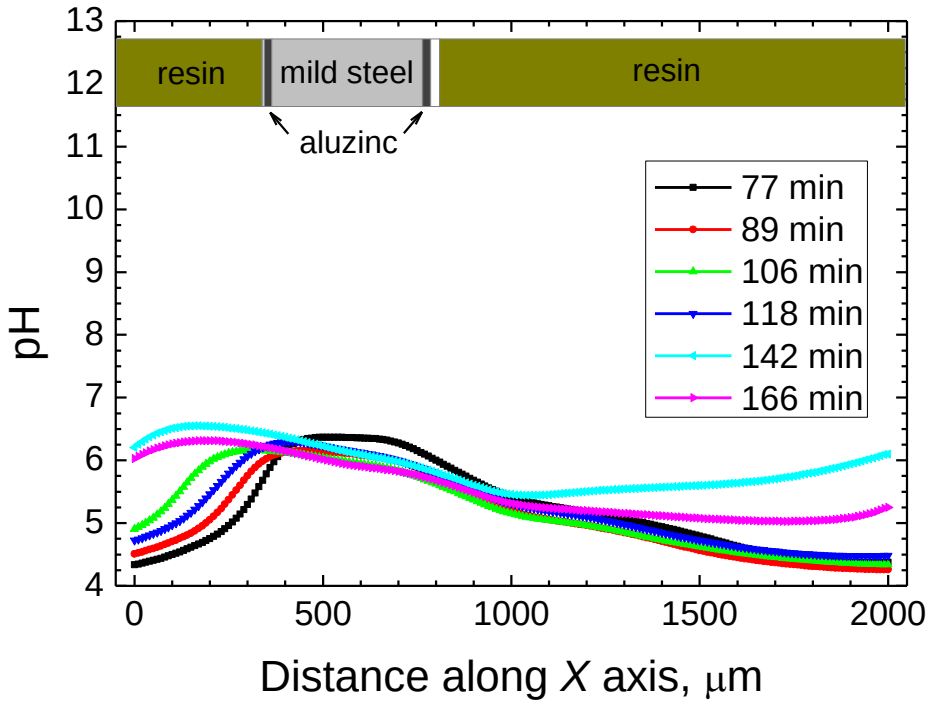

Figure 2. pH distribution above the cut edge in 1 mM NaCl (pH 4.2) measured by potentiometric SECM using an antimony tip. Tip-substrate distance: 15 μm. Scan rate: 7 μm s^{-1}.

Some consideration must be paid to the influence of eventual misalignment of the sample with regards the scanning plane of the probe. Indeed, from the comparison of the current baselines measured over the resin sleeve at either side of the painted cut edge it is observed that there is some tilt of the sample, and the resin part at the right is at a higher level than that at the left. The shorter tip-substrate distance occurring on the resin situated at the right of the exposed cut edge results in smaller tip currents due to greater blockage to diffusion of the redox mediator towards the tip (negative feedback effect). The occurrence of this unavoidable tilt of the sample must be taken in account regarding the redox mediator regeneration over the cut edge itself. In this case, the current measured at the tip corresponds to the regeneration of the redox mediator, and therefore shorter tip-sample distances would lead to an increase in the tip current moving from the left to the right. And this is what it is apparently observed in Figure 1. Yet, the current variation over the tip does not show the same slope at all the immersion times neither shows a monotonous variation as the tip moves towards the right, conversely to what it is observed over the surrounding resin. Therefore, we consider sample tilt not to account for the observed features.

Indeed, pH profiles in Figure 2 correspond well with this behaviour. The solution becomes less acidic than the bulk electrolyte over the cut edge, related to local consumption of protons at the cathodic sites preferentially formed on the steel foil. The pH distributions corresponding to less acidic conditions over the cut edge become broader with the elapse of time, and they extend effectively longer distances over the surrounding insulating resin. But advancement of the local pH variation occurs further into the electrolyte departing from the cut edge towards the right (i.e., moving away

from the aluzinc layer coated with the thicker organic layer), whereas it moves slowly towards the left. This is an indication that only the aluzinc layer at the left is effectively maintaining the anodic reaction and thus dissolves in the electrolyte, whereas that at the right either does not corrode or it does at a slower pace. The asymmetric behaviour of the two metal coated layers only disappears at the longer exposures, resulting from the combined effect of consumption of the aluzinc layer on the left, and effective reduction of the acidity of the small volume of electrolyte in the cell resulting from the consumption of protons in the cathodic reaction. Thus, after 166 min, the bulk electrolyte has attained a pH value close to 6, and slightly more acidic conditions are observed in the proximity of the aluzinc layer at the right that now sustains the anodic process instead. It is also noticeable that the maximum pH values recorded at all times occur between 6 and 7, evidencing the buffering capacity of Zn^{2+} ions in this environment. Precipitation of zinc oxyhydroxides prevents further alkalization of the solution. Though formation of precipitating zinc oxides is thermodynamically favoured when the local solution pH is between 11 and 12 [27], they can precipitate at pH values as low as 6 [27,29].

Experiments using model zinc-iron galvanic pairs [22,24,30] showed alkalization happened above the iron specimen due to reduction of dissolved oxygen (according to equation (1)), whereas acidification occurred on the zinc sample due to the hydrolysis of the metal ions released in the anodic oxidation of the metal according to equations (2) and (3) with values close to 6. Furthermore, variations in local pH around non-painted aluzinc layers applied on steel sheet have been investigated by other groups. Yadav et al. [31] showed that an acidic pH (ca. 2) developed over the metal coating layer during galvanic coupling, and it enhanced the corrosion of this layer due to hydrogen evolution. The low pH was attributed to the dissolution and hydrolysis of Al^{3+} ions from the aluzinc metallic layers. Less acidic pH values were monitored by Alvarez-Pampliega et al. [14] in the case of painted hot-dipped galvanized (HDG) steel. In this case the lowest pH values were ca. 5.0, whereas the presence of aluminium in the metal coating only produced a very mild pH decrease amounting 0.5 units. These values lie within the range of the pH values found for a model zinc-iron couple and for a painted cut edge exposed in natural aerated NaCl solution [26].

3.2. SECM imaging of the cut edge in alkaline environment (pH 9.8)

A different behaviour of the cut edge immersed in the alkaline environment is evidenced by the SECM scan lines depicted in Figures 3 and 4. In this case, progressive activation of the cut edge with the elapse of time occurred during approximately two hours, but the surface is completely inactive after three hours due to surface blockage. Furthermore, the electrochemical activity is observed to be progressively shifted towards the right of the cut edge, resulting also in the shift of the pH maximum over the steel foil towards the right with time. This behaviour is consistent with the progressive blocking of the exposed metal due to precipitation of corrosion products in the alkaline environment. Blockage of the cathodic sites on the steel foil firstly occurs closer to the metal coating layer on the left, and oxygen reduction mainly occurs at further distance from the steel-aluzinc interface at the left. Progressive activation of the aluzinc layer on the right is also observed in this case, resulting in local acidification extending partially above the insulating resin at the right, until effective blocking due to

precipitation occurs on the interface. It is interesting to notice that the local alkalization effect related to the cathodic half-reaction on the steel foil amounts less than 1 pH unit in this case, evidencing that smaller pH changes occur when precipitation of corrosion products hinders the corrosion reaction [27,29].

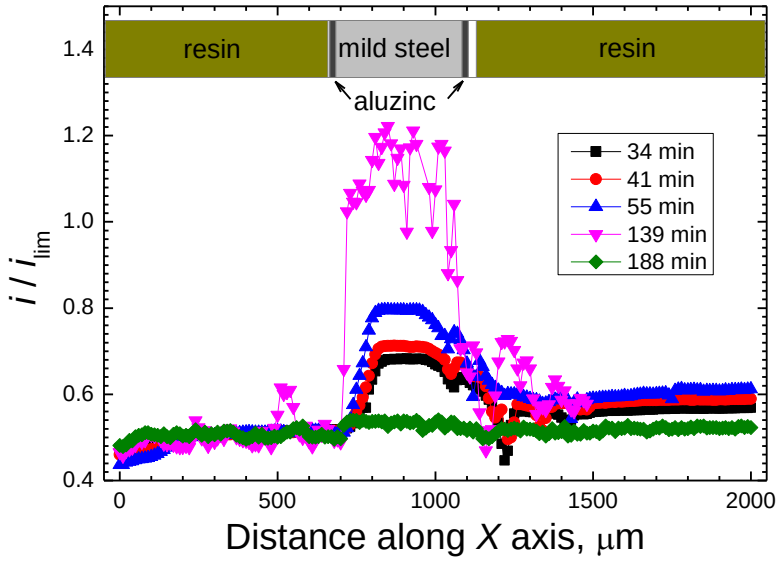

Figure 3. Distribution of electrochemical activity towards regeneration of ferrocene-methanol over a CCS cut edge immersed in 1 mM NaCl (pH 9.8) measured by amperometric SECM using a platinum tip for immersion times indicated in the graph. E_{tip} = +0.50 V vs. Ag/AgCl/(3 M KCl); tip-substrate distance: 15 μm; tip diameter: 10 μm. Scan rate: 7 μm s^{-1}.

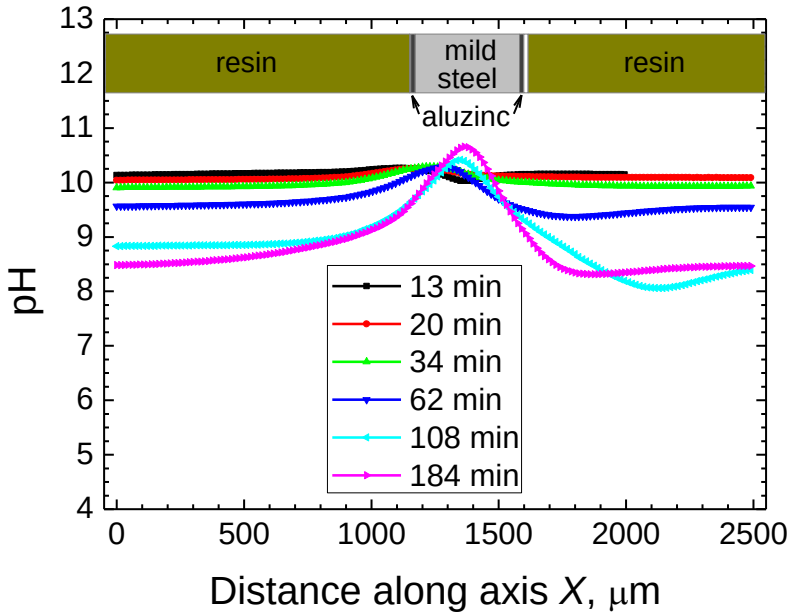

Figure 4. pH distribution above the cut edge in 1 mM NaCl (pH 9.8) measured by potentiometric SECM using an antimony tip. Tip-substrate distance: 15 μm. Scan rate: 7 μm s^{-1}.

3.3. SECM maps of the cut edge

Due to the rather long time required to acquire an SECM image along the complete cut edge exposed to the solution, only one image could be recorded at each pH during the period of maximum electrochemical activity indicated by the scan lines described in Figures 1-4. Therefore, these images can only be considered to be a semi-quantitative description of the system. The SECM images recorded in 1 mM NaCl solutions of pH 4.2 and 9.8 are given in Figure 5. Though the data should be regarded to be rather preliminary data, it is interesting to notice the highly localized nature of the corroding process. Not only differences in electrochemical activity can be observed between the two metal coating layers at either side of the steel foil, but both cathodic and anodic activities are also distributed along each metallic phase as evidenced by the local pH changes in the solution.

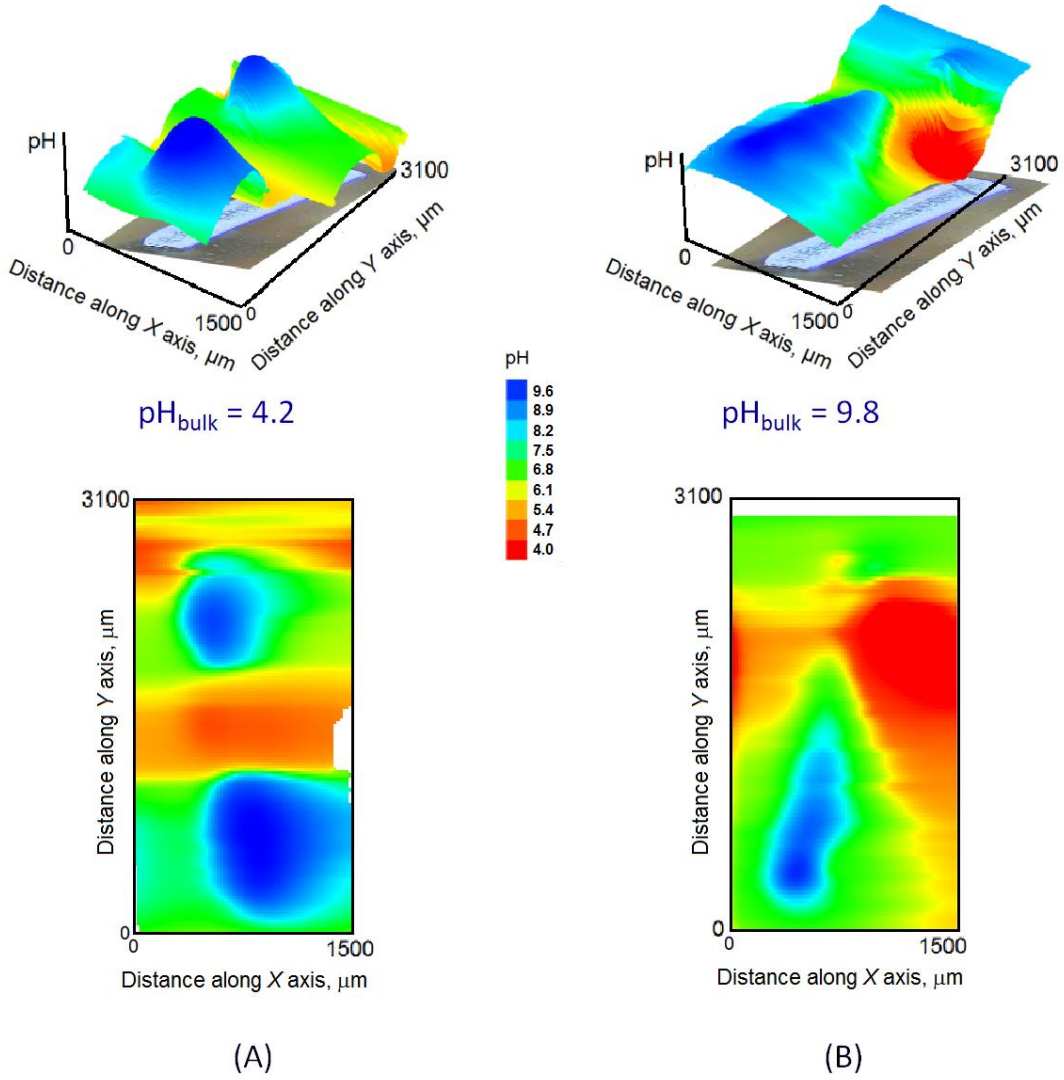

Figure 5. Potentiometric SECM images of pH distributions over the cut edge in: (A) 1 mM NaCl (pH 4.2), and (B) 1 mM NaCl (pH 9.8). Tip-substrate distance: 15 µm. Scan rate: 7 µm s^{-1}.

In the acid solution, most of the cut edge is in contact with an electrolyte with pH values between 6 and 7, due to the buffering ability of soluble Zn^{2+} ions released from the metal coating. Alkaline pH values are only attained around specific sites on the steel foil, and they were not imaged in the sequence of scan lines of Figure 2 that were taken over the central strip across the cut edge (see Figure 5A). Indeed, it can be seen from this image that highest anodic activity corresponding to long exposures is already initiated over the aluzinc layer coated by the thicker polymer coating, and that anodic activity concentrates mainly in the central strip. Thus, cathodic activity on the steel foil is also concentrated in the proximity of that strip, leading to the formation of the two maxima in the image. This map closely resembles previous observations for the cut edge in near neutral solution (cf. Figure 8B in ref. [26]), though in that case more alkaline pH values resulted on the steel foil reaching ca. 10.

A different behaviour is observed in Figure 5B recorded for a cut edge immersed in an alkaline solution. Most of the cut edge remains in contact with alkaline electrolyte close to bulk values, whereas a most anodic activity concentrates in a small fraction of the aluzinc layer, possibly through the development of a corroding pit that is maintained by the high local acidity developed at the site. This local acidity prevents precipitation of corrosion products at this place, and it is responsible for the residual corrosive process over a mainly blocked cut edge. This local anode is also responsible for the lower pH values observed in Figure 4 at the right side of the scan lines recorded at the longer exposures.

We regard these experiments to provide additional support for our proposal of a differential aeration mechanism to describe the time evolution of corrosion processes in embedded cut edge samples detected in near neutral aqueous solution [26]. Dissolved oxygen in the electrolyte has less accessibility to one of the metal coating layers, originating a differential aeration condition leading to enhanced dissolution of aluzinc in this case. This study opens a simpler experimental route to investigate these systems using scanning microelectrochemical techniques, especially SECM in combined potentiometric/amperometric operation compared to freely standing cut edges [1-4]. In this way, changes in the composition, number and size of the different phases forming the cut edge system can be investigated in a systematic way with high chemical and spatial resolution.

4. CONCLUSIONS

- Scanning electrochemical microscopy can be employed to in situ monitor the local distribution of anodic and cathodic sites in a corroding cut edge without significantly altering the corrosion processes by the measurement procedure.
- Embedded samples of asymmetric cut edges can effectively be investigated for differential aeration mechanisms, in order to evaluate the characteristics of the nature and composition of the various materials composing an organic coated coil steel sheet, namely the polymeric coating, the sacrificial metal layers, and the main metal substrate to protect.
- Controlled modification of the pH of the aqueous solution allowed the effects of metal dissolution, buffering ability of the soluble metal ions, and surface blockage by the precipitation of corrosion products on cut edge corrosion to be distinguished.

- Corroding surfaces present acid and alkaline regions, with lower pH values around the metal coating layers. Bulk acid electrolyte promotes a more homogeneous chemical distribution on the cut edge, probably due to hindered precipitation of corrosion products, whereas the amperometric SECM signal increases with immersion time.

ACKNOWLEDGMENTS:
This work has been supported by the Spanish Ministry of Science and Innovation and the European Regional Development Fund under Project No. CTQ2009-14322. Research Training Grants awarded to J.I. by the Spanish Ministry of Economy and Competitivenes (*Programa de Formación de Personal Investigador*), and to B.M.F.-P. by Obra Social La Caixa – Fundación Cajacanarias are gratefully acknowledged. The Agencia Canaria de Investigación, Innovación y Sociedad de la Información and the European Social Funds assisted in meeting the publication costs of this article ("Se agradece la financiación concedida a la ULL por la Agencia Canaria de Investigación, Innovación y Sociedad de la Información, cofinanciada en un 85% por el Fondo Social Europeo").

References

1. D.A. Worsley, H.N. McMurray and A. Belghazi, *Chem. Commun.,* (1997) 2369.
2. D.A. Worsley, H.N. McMurray and S.M. Powell, *Corrosion,* 56 (2000) 492.
3. S. Böhm, H.N. McMurray, S.M. Powell and D.A. Worsley, *Electrochim. Acta,* 45 (2000) 2165.
4. D.A. Worsley, D. Williams and J.S.G. Ling, *Corros. Sci.,* 43 (2001) 2335.
5. H.N. McMurray, S.M. Powell and D.A. Worsley, *Brit. Corros. J.,* 36 (2001) 42.
6. F. Zou, C. Barreau, R. Hellouin, D. Quantin and D. Thierry, *Mater. Sci. Forum,* 289-292 (1998) 83.
7. K. Ogle, V. Baudu, L. Garrigues and X. Philippe, *J. Electrochem. Soc.,* 147 (2000) 3654.
8. K. Ogle, S. Morel and D. Jacquet, *J. Electrochem. Soc.,* 153 (2006) B1.
9. F. Thébault, B. Vuillemin, R. Oltra, C. Allely and K. Ogle, *Electrochim. Acta,* 56 (2011) 8347.
10. F. Thébault, B. Vuillemin, R. Oltra, K. Ogle and C. Allely, *Electrochim. Acta,* 53 (2008) 5526.
11. C. Wagner, *J. Electrochem. Soc.,* 99 (1952) 1.
12. C. Wagner, *J. Electrochem. Soc.,* 104 (1957) 631.
13. F. Thébault, B. Vuillemin, R. Oltra, C. Allely and K. Ogle, *Corros. Sci.,* 53 (2011) 201.
14. A. Alvarez-Pampliega, S.V. Lamaka, M.G. Taryba, M. Madari, J. De Strycker, E. Tourwé, M.G.S. Ferreira and H. Terryn, *Electrochim. Acta,* 61 (2012) 107.
15. T.A. Lowe, G.G. Wallace and A.K. Neufeld, *Corros. Sci.,* 55 (2012) 180.
16. R.M. Souto, B. Normand, H. Takenouti and M. Keddam, *Electrochim. Acta,* 55 (2010) 4551.
17. M.B. Jensen and D.E. Tallman, in: *Electroanalytical Chemistry: a Series of Advances*, vol. 24, A.J. Bard and C.G. Zoski (Eds.); CRC Press: Boca Raton FL (2012), p. 171.
18. G. Denuault, G. Nagy and K. Toth, in: Scanning electrochemical microscopy, 2nd edn, A.J. Bard and M.V. Mirkin (Eds.); CRC Press: Boca Raton FL (2012), p. 275.
19. R.M. Souto, A. Kiss, J. Izquierdo, L. Nagy, I. Bitter and G. Nagy, *Electrochem. Commun.,* 26 (2013) 25.
20. J. Izquierdo, L. Nagy, I. Bitter, R.M. Souto and G. Nagy, *Electrochim. Acta,* 87 (2013) 283.
21. J. Izquierdo, A. Kiss, J.J. Santana, L. Nagy, I. Bitter, H.S. Isaacs, G. Nagy and R.M. Souto, *J. Electrochem. Soc.,* 160 (2013) C451.
22. J. Izquierdo, L. Nagy, Á. Varga, J.J. Santana, G. Nagy and R.M. Souto, *Electrochim. Acta,* 56 (2011) 8846.

23. J. Izquierdo, L. Nagy, Á. Varga, I. Bitter, G. Nagy and R.M. Souto, *Electrochim. Acta,* 59 (2012) 398.
24. J. Izquierdo, L. Nagy, S. González, J.J. Santana, G. Nagy and R.M. Souto, *Electrochem. Commun.,* 27 (2013) 50.
25. J. Izquierdo, L. Nagy, J.J. Santana, G. Nagy and R.M. Souto, *Electrochim. Acta,* 58 (2011) 707.
26. B.M. Fernández-Pérez, J. Izquierdo, S. González and R.M. Souto, *J. Solid State Electrochem.,* 18 (2014) 2983.
27. S. Thomas, N. Birbilis, M.S. Venkatraman and I.S. Cole, Corrosion of zinc as a function of pH, *Corrosion,* 68 (2013) 015009.
28. R.M. Souto, J. Izquierdo, J.J. Santana, A. Kiss, L. Nagy and G. Nagy, in: *Current Microscopy Contributions to Advances in Science and Technology*, editado por A. Méndez-Vilas (Ed.); Formatex Research Center: Badajoz (2012), p. 1407.
29. T.H. Muster and I.S. Cole, *Corros. Sci.,* 46 (2004) 2319.
30. E. Tada, K. Sugawara and H. Kaneko, *Electrochim. Acta,* 49 (2004) 1019.
31. A.P. Yadav, H. Katayama, K. Noda, H. Masuda, A. Nishikata and T. Tsuru, *Electrochim. Acta,* 52 (2007) 2411.